

Parameter Sensitivity Analysis for Design and Control of Tendon Transmissions

Vincent Hayward and Juan Manuel Cruz-Hernández

McGill University
Center for Intelligent Machines
3480 University Street
Montréal, Québec, Canada, H3A 2A7

Abstract

We apply sensitivity analysis to the design and control of a tendon transmission. With this approach, some preferred values for the system parameters and a feedback compensator can be proposed. The controller has the special characteristic of being designed based on a linear plant using a robust loopshaping technique, yet it compensates also for the nonlinear behavior of the plant, while exhibiting good disturbance rejection and robustness. Experimental results using a test bench are discussed.

1. Introduction

There is freedom in the design of tendon transmissions. The question arises of how to choose the design parameters to improve performance. To answer this, we select performance objectives which are relevant to a haptic device¹ [7]— and look at the sensitivity of the parameters with respect to the performance objectives. These include extending the frequency response to the widest range possible, as well as reducing friction and inertia as experienced from the load side of the transmission.

The design of the compensator would be straightforward if a linear model could be used. Unfortunately, a transmission exhibits friction, so precise control requires the compensation of non-linear friction effects. We will develop a scheme which can be tuned for a wide class of systems and which neither rely on a detailed knowledge of the non-linear behavior of friction, nor requires measurement of velocity.

The purpose of the tendon drive is to transmit mechanical signals from a remote location so that the actuators can be mechanically grounded. Because mechanical signals are transmitted by taking advantage of the cohesive forces in a material, large amounts of energy can be transmitted by small amounts of material. This is why cable and tendon transmissions have been a technique of choice for the implementation of teleoperators, hand controllers and now haptic devices for almost five decades, [6, 10, 2].

The transmission is of type 2N [8], with two actuators per channel. This type of transmission minimizes the average tension, while reducing stresses in the supporting structure and idler pulleys. It results in lower friction, simplified assembly and

¹A haptic device may be viewed as a high fidelity force reflecting hand controller

Friction in tendon drives tends to grow linearly with tension. Remark first that if we look at friction as noise on mechanical signals, we see that it will grow with the intensity of the force signal. Consider now the function of a haptic device which is to display signals to the hand of an operator. Displacements, forces and other mechanical sensations, obey the same laws as other sensations, following a Fechnerian scale expressed, for example, by a Weber fraction $\Delta I/I$, where I is the intensity of the stimulus. This means that the sensitivity to changes in the signal (noise here) decreases with the signal intensity, in other terms, the relative sensitivity is constant. The mechanical signal-to-noise ratio in a transmission of type 2N can be made roughly constant across its dynamics range instead of decreasing with the signal intensity as in a conventional transmission.

Analogously to class B electronic power amplifiers, each motor is driven by a half-wave signal, as illustrated in Figure 1. Practice has shown that the switching

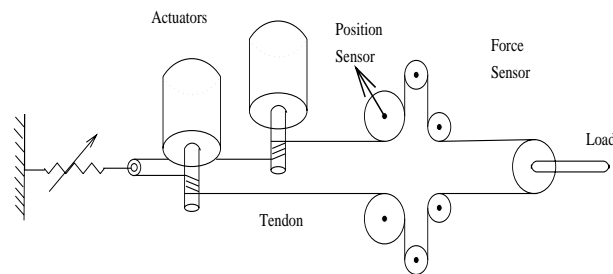


Figure 1. Transmission structure.

nature of the signal did not cause significant distortion, provided that the stiffness of the proximal portion of the transmission is sufficiently high to prevent excessive amounts of stored elastic energy. The generation of the actuator signal was simply accomplished using clamping diodes on the path of a single current amplifier shared by the two actuators. The current amplifier (linear amplifier) effectively inverts by feedback the electrical transfer function (roughly an RL circuit) of the actuators and insures that current, and therefore torque, tracks precisely the input control signal across a bandwidth much larger than the mechanical bandwidth of the drive.

Displacement and force are measured directly on the tendon path via optical sensors developed in our laboratory. Both rely on differential measurements of infrared light intensities sensed by PIN diodes. This type of sensor has the usual benefits of optical sensing techniques — that of absence of contact, low noise, immunity to environmental conditions and EMF perturbations.

2. Model

Figure 2 illustrates an engineering model of the plant. It includes the inertia of the motor I_M , linear damping lumped into damper B , r the pulley ratio between a capstan and a driven pulley, k_1 the elasticity of the proximal section of the transmission, k_2 the elasticity of the distal part, I_c the inertia of the driven manipuladum, and Z_H an arbitrary impedance representing the load, an operator's hand for example. We call

$$k_e = (k_1 k_2) / (k_1 + k_2), \quad (1)$$

a factor expressing the degree of “co-location” of the force measurement.

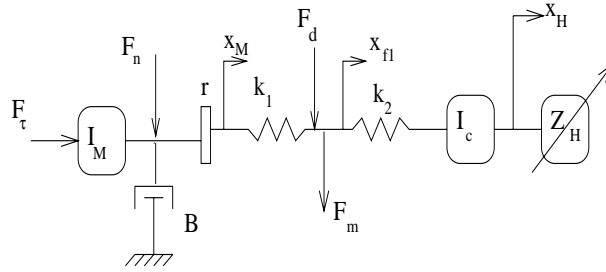


Figure 2. Model of the plant.

transmission of force from the actuator to the load, the transfer function can be worked out for both the actuator force and the actuator friction signal. For the rest of this paper, the variable load will be simplified to a single elasticity k_z , which can be viewed as a worst case as far as stability is concerned:

$$\frac{F_m}{F_\tau} = \frac{F_m}{F_n} = \frac{N(s)}{D(s)} = \frac{k_e I_c s^2 + k_z k_e}{r^2 I_M I_c s^4 + r^2 I_c B s^3 + (k_e I_c + r^2 I_M (k_z + k_e)) s^2 + r^2 B (k_e + k_z) s + k_z k_e} \quad (2)$$

The disturbance friction signal due to the transmission and seen by the sensor is:

$$\frac{F_m}{F_d} = \frac{r^2 I_M I_c}{D(s)} \quad (3)$$

3. Analysis

3.1. Effect of r

A first remark is in order: the numerator of the transfer function (3) is highly sensitive to r and independent from frequency. Increasing r is equivalent to increasing the apparent inertia of the actuator as far as the transmission is concerned. The counter-intuitive result here is: the higher the actuator inertia, or equivalently the higher the pulley (or gear) ratio is, the better the friction disturbance rejection is. This can be understood from another perspective, considering that for a given desired output signal and a given disturbance, a more inert actuator (or higher ratio) will demand a larger input signal, improving the signal-to-noise ratio. The trade-off is as follows: if the ratio is made too high, the actuator might saturate. The other downside of increasing the ratio is the increase of apparent inertia when the transmission is backdriven. However, since force feedback is applied, the apparent inertia is divided by the loop gain. Thus, an optimal design will result from the the highest possible ratio that will not saturate the actuator and which will permit the highest loop gain possible for a given desired phase margin, since r appears in the denominator of the transfer functions. On the upside, a high ratio will increase the peak force generated by the system. In the prototype, the actuator shafts are directly driving the tendons with no intervening capstans and r is close to 15:1.

To understand the effect of the sensor placement, the sensitivity function $S_{k_1}^G$ in the frequency domain with respect to k_1 was computed for various values of k_1 , while the other parameters were set to values close to those of the actual prototype.

$$S_{k_1}^G = \frac{(r^2 I_M I_c^2 s^6 + r^2 I_c^2 B s^5 + 2r^2 I_c I_M k_z s^4 + 2r^2 I_c B k_z s^3 + r^2 I_M k_z^2 s^2 + r^2 B k_z^2 s) \frac{k_2^2 k_1}{(k_1 + k_2)^2}}{r^2 I_M I_c^2 s^6 + r^2 I_c^2 B s^5 + (k_e I_c (k_e I_c + r^2 I_M (k_e + 2k_z))) s^4 + r^2 B k_e I_c (k_e + 2k_z) s^3 + k_z k_e (2I_c k_e + r^2 I_M (k_z + k_e)) s^2 + r^2 B k_z k_e (k_e + k_z) s + k_z^2 k_e^2} \quad (4)$$

It can be seen in Figure 3 that a soft transmission with a stiff end portion ($k_1 \gg$

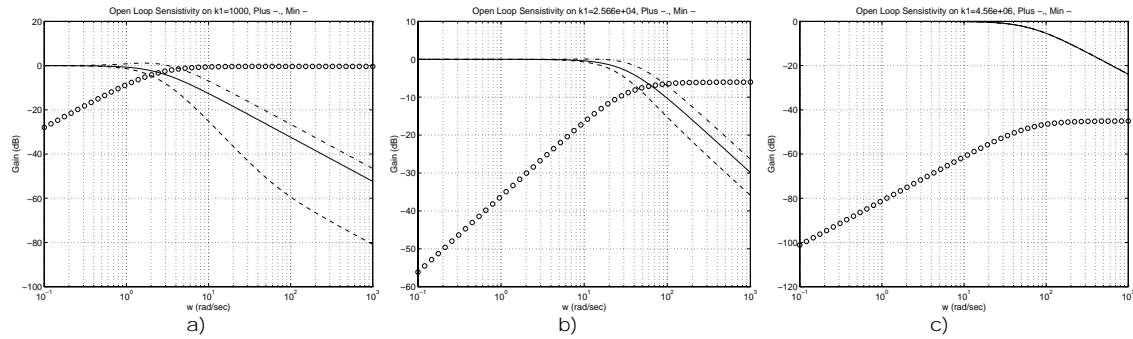


Figure 3. Plots for the transfer function, sensitivity function, and $G(s)(1 \pm S(s))$ with respect to k_1 . Notation: Sensitivity function $S(s) \circ \circ \circ$, Transfer Function $G(s) -$, $G(s)(1 + S(s)) - . . .$, $G(s)(1 - S(s)) - - -$.

a) $k_1 = 1 * 10^3$, b) $k_1 = 2.566 * 10^4$, c) $k_1 = 4.56 * 10^6$

k_2) is very sensitive in the high frequencies to slight changes in k_z , while a stiff transmission with a soft end-portion, not only increases the response's bandwidth but also decreases the sensitivity to very small values. It can be concluded that k_e expressing the degree of collocation of the force sensor has a major influence on the ability for a transmission to be force-controlled.

This k_e -dependence has been noticed by many researchers while implementing force control on a manipulator [4]: a stiff force sensor clamped at the wrist and separated from the actuator by a soft transmission will make the control difficult, and if at all possible, the response will either be highly sensitive to the load variations (hence the hard contact bouncing so often discussed) or effective only in the very lowest range of the frequency domain. A force sensor located near the actuator and separated from the load by the structural elasticity of the manipulator has exactly the opposite property: the sensitivity to the load is low (so a single tuning will work for a wide range of loads but disturbance rejection is less good so it cannot be precise) and the response range is wide.

A parallel can be drawn between the effect of a gear ratio for position control and the effect of k_e in force control. A high gear ratio makes the position control insensitive to load variations and other disturbances (so it is easy to control), while a direct drive robot will be maximally sensitive to the same factors (so it can be accurate and the disturbance rejection can be good but is hard to control). From that viewpoint we may see that the co-location factor k_e plays for force control a role analogous to r for position control.

Damping B is important because this will inform the designer with the effect of changes of properties of the transmission.

$$S_B^G = \frac{-Br^2s(I_c s^2 + (k_e + k_z))}{r^2 I_M I_c s^4 + r^2 I_c B s^3 + (k_e I_c + r^2 I_M (k_z + k_e))s^2 + r^2 B (k_e + k_z)s + k_z k_e} \quad (5)$$

The sensitivity curves for the nominal plant parameter values are extremely similar to the curves produced by k_e , so they are not reproduced here. The plant response is obviously mostly affected in the vicinity of the cut-off frequency (where half of the input signal is dissipated). The conclusion is evident: damping should be low and if it must be high, small changes will have big effects on the plant's response, possibly destabilizing the closed loop response.

3.4. Effect of k_z

We now consider the effect of load changes on the response.

$$S_{k_z}^G = \frac{k_z (k_z^2 r^2 I_M s^2 + k_e^2 r^2 B s)}{r^2 I_M I_c^2 s^6 + r^2 I_c^2 B s^5 + (k_e I_c (k_e I_c + r^2 I_M (k_e + 2k_z)))s^4 + r^2 B k_e I_c (k_e + 2k_z)s^3 + k_z k_e (2I_c k_e + r^2 I_M (k_z + k_e))s^2 + r^2 B k_z k_e (k_e + k_z)s + k_z^2 k_e^2} \quad (6)$$

It is seen in Figure 4 that the sensitivity to this parameter is very high for small

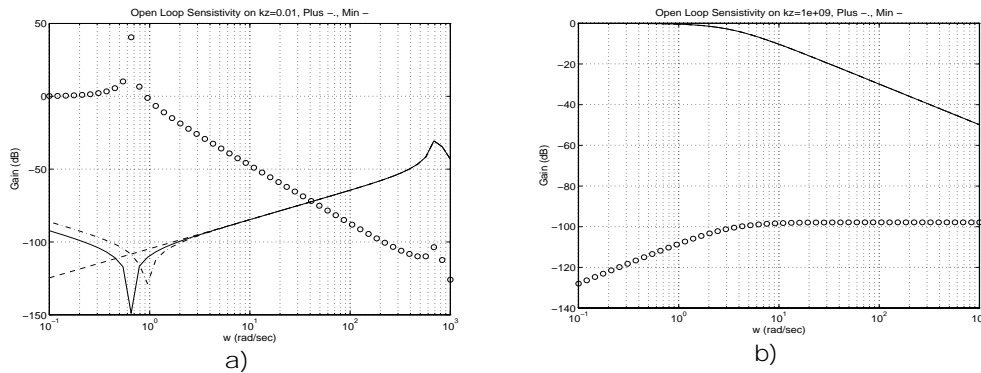


Figure 4. Plots for the transfer function, sensitivity function, and $G(s)(1 \pm S(s))$ with respect to k_z . Notation: Sensitivity function $S(s)$ $\circ \circ \circ$, Transfer Function $G(s)$ —, $G(s)(1 + S(s))$ - - - -, $G(s)(1 - S(s))$,
 a) $k_z=0.01$, b) $k_z=1 * 10^9$

values, while it vanishes at high values. While this may seem obvious in retrospect, it is important to notice that the sensitivity has a resonant shape with the peak in the vicinity of the plant's first natural resonance. This can be seen in (2), the independent term, both in the numerator and the denominator, depends on k_z , so if k_z is small, the plant will have two zeros and one pole.

This means that the response is essentially unknown when the load is stiff. As a consequence it is imperative to consider feedback control to reduce sensitivity. The closed loop transfer function is as follows:

$$T(s) = \frac{k_e I_c s^2 + k_z k_e}{r^2 I_M I_c s^4 + r^2 I_c B s^3 + (k_e I_c (1+K) + r^2 I_M (k_z + k_e))s^2 + r^2 B (k_e + k_z)s + k_z k_e (1+K)} \quad (7)$$

Recall that for a closed loop transfer function, where α is some parameter under study, $S_\alpha^T = S_G^T S_\alpha^G$ [5]. Since S_α^G was computed for B and k_z we only need to

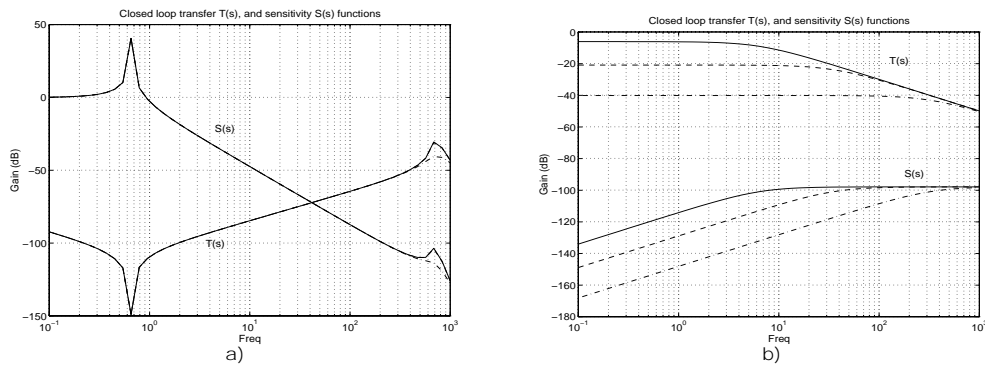


Figure 5. Plots for the transfer function $T(s)$ and sensitivity function $S(s)$ respect to k_z . a) $k_z = 0.01$, and b) $k_z = 10^9$ for a constant controller with values 1, 10, 100. Notation: $K=1$ —, $K=10$ - - -, $K=100$ -.-.-.

could be a lead compensator of the form $C(s) = (s + z)/(s + p)$, it can be found that the sensitivity function becomes:

$$S_G^T = \frac{(s + p)D(s)}{(s + p)D(s) + (s + z)N(s)} \quad (8)$$

Now, any change in p or z will affect sensitivity in the same order as a simple gain K with the disadvantage of complicating tuning.

3.5. Conclusion about design

In the absence of further information about the exact nature of the plant, the simple gain controller K should be preferred over a complex controller composition. This simple controller will improve the response, and decrease the sensitivity, while its tuning is particularly simple. The tuning will only involve raising the value of K under the worst conditions (smallest needed k_z) until the closed loop stability is compromised, while observing the response in the time domain, for example.

This is further indicative of the fact that the plant's non-linearities in fact play an important role in the system's response, and this vindicates the use of a single gain controller in the absence of additional information.

4. Controller Design

We now consider the design of a less conventional controller designed for the plant described in the previous section with a goal of improving the extent and the precision of the response of the system, and reducing the apparent friction of the transmission when it is back driven as well as the apparent inertia.

The input-output behavior of the tendon transmission, although complicated because of the presence of non-linearities, might in fact be viewed as the combination of simpler subsystems, which once combined create an apparently complicated behavior. For illustration, Figure 6, shows the input force to output force relationship exhibiting a complex hysteretic behavior. A possible decomposition is suggested by

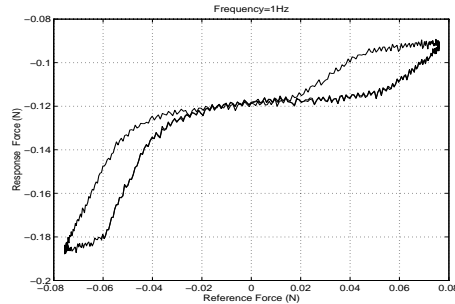


Figure 6. Hysteretic behavior of the plant.

the physical nature of the plant. The transmission includes a linear system representing elasticity, damping and inertia of its mechanical components. This was verified by measuring the transfer function of the system and then observing that the response is indeed well defined, including resonant characteristics that could be precisely identified for a given input amplitude. However, the dependency of the response with respect to the input presented the hallmarks of nonlinear characteristics such that, the linear part is camouflaged by the nonlinear distortion. Figure 7 shows in fact how the response may present a resonant peak shifting from 15 Hz to 30 Hz depending on the amplitude of the input. The response is nevertheless precise and was found not to change with time. This response was experimentally obtained with a very stiff load which is the worst case as shown in the previous section.

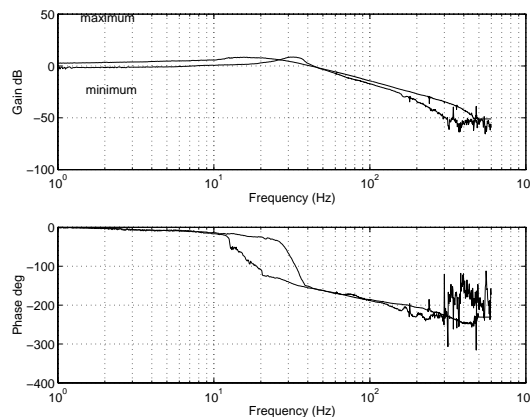


Figure 7. Open loop Bode plot.

It was further verified that nonlinear stiffening of the material used to make the tendons, a possible source of non-linearity, was not significant. The other likely cause for a non-linear response is obviously friction. Friction has been extensively studied and various models have been proposed. The reader is referred to the extensive

It was said that friction increases roughly linearly with the tendon tension. But more importantly, the observed friction does not exhibit noticeable stiction, often referred to as Stribeck friction. From this observation we can conclude that no significant potential energy is being stored by the occurrence of the friction phenomenon per se; only dissipation occurs. It can therefore be considered as memoryless and thus can be completely represented as a single valued input-output relationship.

In this paper, we adopt a simple representation of friction: the standard “break-away” model. With this model, a transmission is an input-output device transmitting torque (or force), while motion is not considered explicitly. A force balance equation states that the transmission transmits the input torque to the output torque minus a torque lost in dissipation, with the exception that when the input torque is under a threshold (under the breakaway level), no torque is transmitted to the output (since no motion is observed) and the friction balances exactly the input torque. This results in an input-output force-force friction model represented as a dead-band as seen in Figure 8, which is a single valued relationship. The exact nature of this curve, whether it is even dependent or not from some other parameters is irrelevant to the rest of this discussion. All what matters is that its slope varies with the input. It is well known that an input-output non-linear relationship of

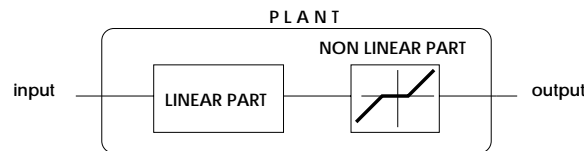


Figure 8. Plant representation: Wiener model [11]

the type just described can easily be “straightened” with the application of simple gain feedback and that no stability problem may occur since the closed loop system has no memory, no energy is stored. However, any controllers having dynamics, for example a PD, a PI, or any other filter for that matter, are liable to create complex behaviors including instabilities, limit cycles, or even chaotic patterns [9].

Returning to the physical structure of the transmission, recall that we may view it as a linear system resulting from a combination of springs, dampers and inertias forming a low pass filter, cascaded with a single valued deadband-like nonlinear relationship. Such a combination will certainly create a hysteretic-like behavior. This can easily be seen by considering a ramping input: while in the deadband, no signal is observed at the output; this has the effect of shifting the response on the right. When the input reverses, the system enters the deadband again, shifting the response to the left, and so on, forming a hysteresis-like loop.

4.2. Controller Synthesis

Recall that another objective is to extend the frequency response as far as possible, thus the transmission has to be stiffened by feedback. From the previous discussion, this also has the effect of correcting the hysteretic-like behavior of the plant.

4.3. Experimental Single Gain Controller

The experimental closed loop Bode plot is shown in Figure 9. As predicted by the previous analysis, it has a marked resonant characteristic. The tuning is trivial, a phase margin is chosen, and the gain follows from this choice. It must be said that despite the low pass nature of the transmission, an effective apparent friction

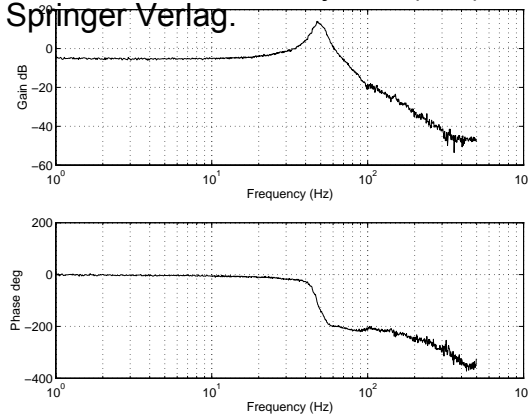


Figure 9. Closed loop Bode plot of the force response with a proportional controller.

reduction is achieved. The usable frequency range, which was 40 Hz open loop, is slightly improved. It is robust and noise free.

4.4. Approximate Plant Inversion

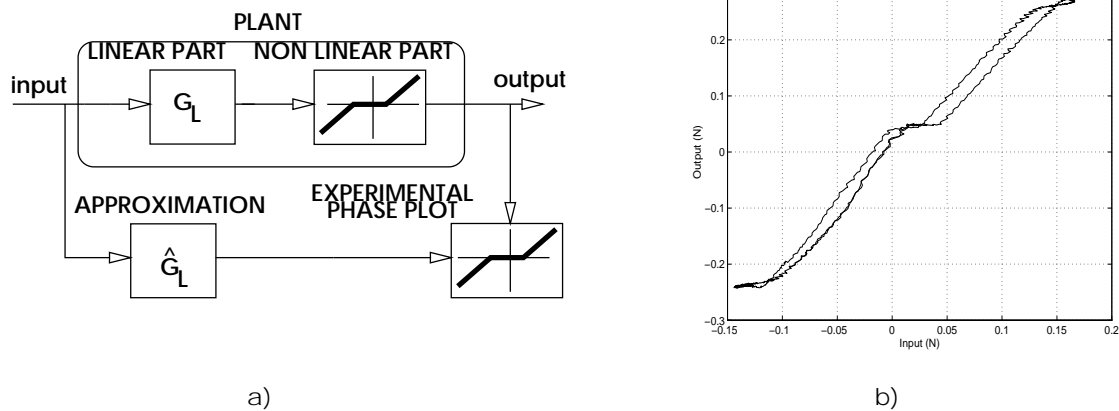


Figure 10. a) Theoretical representation, and b) Experimental phase plot at low velocity, $F = 0.2$ Hz and small amplitude: 0.31 N

Referring to Figure 10.a), the objective is to cancel the low pass dynamics of the plant in order to achieve stiffening, so that the feedback will only see a uni-valued input output relationship. This concept is represented in Figure 11. In order to verify that the transfer function actually decomposes in the needed fashion, a model $\hat{G}_L(s)$ of the plant is identified (using conventional identification methods) and the same input (of various kinds) is presented to the plant and to the model. The phase plot of the plant output is traced against the output of the model. The optimal model will minimize the area of the phase plot at all frequencies. See Figure 10.b) for the experimental result. Once the model is found, the ideal controller is simply $\hat{G}_L^{-1}(s)$; however, since the plant is lowpass, it would not have a proper transfer function and would not be realizable. We must therefore settle for an approximate inverse in the desired frequency range and poles are added to achieve this.

The resulting pole-zero cancellation control is effectively a non-robust design since it relies on a precise identification of the plant. In fact, because of its uncertain

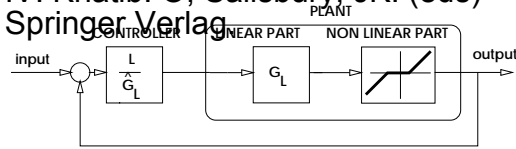


Figure 11. Loopshaping technique.

non-linearities, such identification is not possible.

Loopshaping technique was used to design a feedforward controller [3]. The idea, as is well known, is to choose a loop transfer function $L(s)$ so that we can achieve a robust performance, good robustness with $T(s)$ small at high frequencies, and disturbance rejection at low frequencies making S_G^T small, which is sometimes not possible to achieve just by modifying the system parameters. The condition to design a controller with robust performance are to have an internally stable plant and to enforce the following inequality:

$$\| |W_1 S| + |W_2 T| \|_\infty < 1 \quad (9)$$

W_1 is a weighting function used to determine internal stability by enforcing nominal performance such that $\|W_1 S\|_\infty < \epsilon$, where ϵ is the maximum amplitude of the error signal over the whole frequency range. W_2 is another weighting function to enforce robust stability, $\|W_2 T\|_\infty < 1$. T is the closed loop transfer function and S the sensitivity function S_G^T . $L(s)$ can then be determined using a graphical method.

The controller $C(s)$ is obtained from $C(s) = \frac{L(s)}{P(s)}$, with $P(s) = \hat{G}(s)$. Again, the controller has to be proper and internal stability of the plant has to be ensured. This method is suitable for our purpose since the plant $G(s)$ is stable and minimum phase, as can be seen in Figure 7, and has all its poles and zeros in the right half plane. We chose $L(s)$ to behave as a second order system of the form:

$$L(s) = \frac{\omega_n^2}{s^2 + 2\zeta\omega_n s + \omega_n^2} \quad (10)$$

with a natural frequency $\omega_n = 40Hz$, and $\zeta = 0.5$. This can be considered as a good response in open loop and is what we can expect for this plant. Physically the plant may not achieve more than a few Hertz beyond its original natural frequency, for this reason we did not place the response of $L(s)$ further than 40Hz. Furthermore, in closed loop the bandwidth will increase. As we demonstrated experimentally, we can achieve almost the same bandwidth for an $L(s)$ with $\omega_n = 40Hz$ than for $\omega_n = 80Hz$. The difference is that the closed loop response has dithering behavior when we used a higher ω_n . This happens because we are amplifying the noise that appears after 40 Hz, and because we were breaking the condition needed to achieve a robust performance as specified by the loopshaping technique. The controller was designed using an approximation to the plant obtained with a large input amplitude, when nonlinear disturbance is minimized. It was also shown to be effective for all amplitudes. The experimental response of the system in closed loop using the controller described above is presented in Figure 12, where it can be observed that no matter which amplitude of the input we give to the closed loop system, the result is always almost the same, and also a very good noise rejection is achieved. The range of uncertainty (Figure 7) in amplitude was quite large, and now this range has been reduced for most of the low frequency, which for haptic interfaces is crucial.

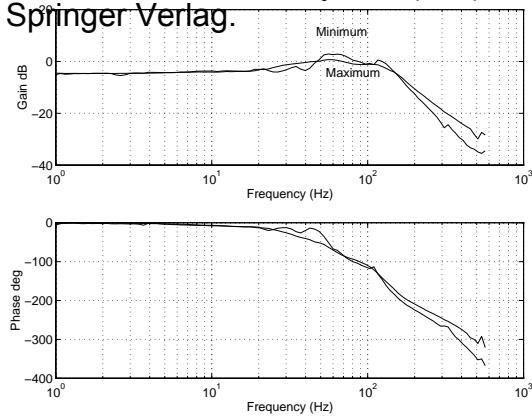


Figure 12. Closed loop Bode plot using $C(s) = \frac{L(s)}{P(s)}$.

We can look at the input-output relation of the closed loop system and compare how this behavior has been modified, see Figure 13.a. The deadband presented in

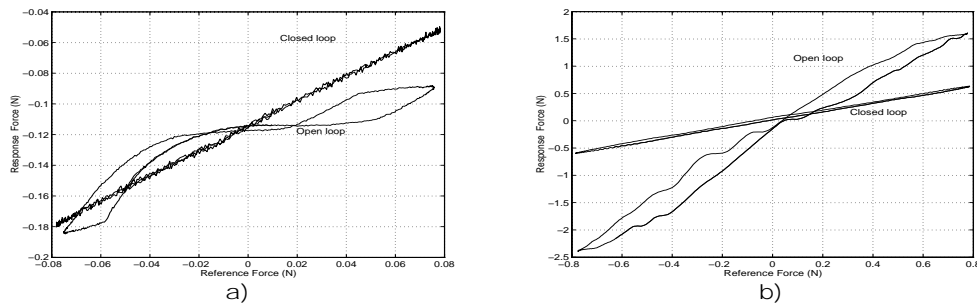


Figure 13. Comparison of open and closed loop. a) Small amplitude and $F=0.2$ Hz., and b) Large amplitude and $F=1$ Hz.

open loop as well as the hysteresis-like behavior is corrected to give a linear behavior. We present another curve of higher amplitude and different frequency as in Figure 13.b. The small area that appears in the closed loop signal is due to some phase shift between the input and the output and is not due to hysteresis. We have been able to improve the system response and compensate for nonlinearities, not just for some frequencies but for a wide range of them.

5. Conclusion

A model for tendon transmissions was presented. An extensive sensitivity analysis was carried out to understand how the parameters affect the behavior of the system. It was found that for the value of r , a tradeoff between friction rejection, inertia reduction and saturation in the actuator has to be achieved. k_e (the force dividing factor) was found to be an expression of the degree of collocation of the force sensor along the transmission. Sensitivity analysis enable us to show the effects of collocation on a transmission ability to transmit forces. The effect of a variable load k_z can be reduced only by a feedback controller. The proportional controller is the only one which can reduce the sensitivity function S_G^T , without any complicated tuning.

The final design of the controller was done using the loopshaping technique, to

in *Experimental Robotics IV*, Khatib, O., Salisbury, J.K. (eds), LNCIS 223, pp. 241-252, Springer Verlag.

plant were presented. This controller, because of its robustness and disturbance rejection, compensates for the nonlinearities that appeared in open loop and also reduces the uncertainty range of the response.

6. Acknowledgments

Initial funding for this project was provided by a research contract with the Canadian Space Agency (No. 9F009-1-1441/01-SR). Major funding is now provided by the project "Haptic Interfaces for Teleoperation and Virtual Environments" (AMD-5) funded by IRIS (second phase), the Institute for Robotics and Intelligent Systems part of Canada's National Centers of Excellence program (NCE). Additional funding was from an operating grant from NSERC, the National Science and Engineering Council of Canada.

The second author would like to acknowledge the generous support of Universidad Nacional Autónoma de México (UNAM) in the form of a postgraduate fellowship.

The authors wish to acknowledge contributions of Christopher Strong, Xianze Chen, and Jan Sinclair from MPB technologies Inc., Montreal, Canada.

References

- [1] Armstrong-Helouvry, B. Dupont, P. Canudas De Wit, C. 1994. Survey of models, analysis tools and compensation methods for the control of machines with friction, *Automatica* 30(7), pp. 1083-1138.
- [2] Bejczy, A. K., Salisbury, K. 1980. Kinesthetic coupling between operator and remote manipulator. Proc. *International Computer Technology Conference, ASME*, San Francisco, pp. 197-211.
- [3] Doyle, John C., Francis, B. A., Tannenbaum A. R. 1992. *Feedback Control Theory*. New York: Maxwell Macmillan International.
- [4] Eppinger, S.D. and Seering, W.P. 1987 Understanding Bandwidth Limitations in Robot Force Control. Proc. *IEEE International Conference on Robotics and Automation*, Vol. 1, pp. 904-909.
- [5] Frank, P. M. 1978. *Introduction to sensitivity analysis*. Academic Press.
- [6] Goertz, R. C., Thompson, W. M. 1954. Electronically controlled manipulator. *Nucleonics*, 12(11), pp. 46-47.
- [7] Hayward, V. 1995. Toward a seven axis haptic interface. *IROS'95, Int. Workshop on Intelligent Robots and Systems*. pp. 133-139.
- [8] Jacobsen, S.C. and Ko, H. and Iversen, E.K. and Davis, C.C. 1989 Control Strategies for Tendon-Driven Manipulators Proc. *International Conference on Robotics and Automation*, Vol. 1, pp. 23-28,
- [9] Townsend, W.T., Salisbury S.K. The effect of Coulomb friction and stiction on force control. Proc. *IEEE Conference on Robotics and Automation*, pp. 883-889.
- [10] Vertut, J. 1976. Advance of the new MA 23 force reflecting manipulator system. Proc. *2nd International Symposium on the Theory and Practice of Robot and Manipulators*, CISM-IFTToMM, pp. 307-322.
- [11] Wiener, N. 1958. *Nonlinear problems in random theory*. New York: The Technology Press of The Massachusetts Institute of Technology and John Wiley and Sons, Inc.